https://doi.org/10.5194/bg-2022-214
Preprint. Discussion started: 9 November 2022

Biogeosciences Discussions

Physical and stoichiometric controls on stream respiration in a headwater stream

Jancoba Dorley[1], Joel Singley[2,3], Tim Covino[4,5], Kamini Singha[6], Michael Gooseff[7,8], Ricardo González-Pinzón[1]

Correspondence to: Ricardo González-Pinzón (gonzaric@unm.edu)

[1]Civil, Construction and Environmental Engineering, University of New Mexico, Albuquerque, NM USA
[2]Environmental Studies Program, University of Colorado, Boulder, CO USA
[3]Biology, Marine Biology, and Environmental Science, Roger Williams University, Bristol, RI USA
[4]Ecosystem Science and Sustainability, Colorado State University, Fort Collins, CO USA
[5]Department of Land Resources and Environmental Sciences, Montana State University, Bozeman, MT USA
[6]Geology and Geological Engineering, Hydrologic Science and Engineering Program, Colorado School of Mines, Golden, CO USA
[7]Civil, Environmental and Architectural Engineering, University of Colorado, Boulder, CO USA
[8]Institute of Arctic and Alpine Research, University of Colorado, Boulder, CO USA

Abstract. Many studies in ecohydrology focusing on hydrologic transport argue that longer residence times across a stream ecosystem should consistently result in higher biological uptake of carbon, nutrients, and oxygen. This consideration does not incorporate the potential for biologically mediated reactions to be limited by stoichiometric imbalances. Based on the relevance and co-dependences between hydrologic exchange, stoichiometry, and biological uptake, and acknowledging the limited amount of field studies available to determine their net effects on the retention and export of resources, we quantified how microbial respiration is controlled by the interactions and supply of essential nutrients needed (C, N, P) in a headwater stream in Colorado, USA. For this, we conducted two rounds of nutrient experiments, each consisting of four sets of continuous injections of Cl- as a conservative tracer, resazurin as a proxy for aerobic respiration, and one of the following nutrient treatments: a) N, b) N+C, c) N+P, and d) C+N+P. Nutrient treatments were considered as known system modifications to alter metabolism, and statistical tests helped identify the relationships between hydrologic transport and respiration metrics. We found that as discharge changed significantly between rounds and across stoichiometric treatments, a) transient storage mainly occurred in side pools along the main channel and was proportional to discharge, and b) microbial respiration remained similar between rounds and across stoichiometric treatments. Together, our results indicate that residence time alone could be a weak predictor of stream respiration due to the relevance of local and dynamic variations in stoichiometric conditions.

1 Introduction

High biochemical processing rates in streams and rivers occur at locations and times where the dynamic interconnections among hydrologic exchange, residence time, nutrient supply, and microbial biomass combine to form optimum conditions for metabolic activity (i.e., the transformation of nutrients, carbon, and oxygen or another

https://doi.org/10.5194/bg-2022-214
Preprint. Discussion started: 9 November 2022


Biogeosciences Discussions Open Access EGU

electron acceptor into energy and biomass). The exchange of water between the main channel and transient storage zones, where most microbes exist, is the primary mechanism supplying carbon, nutrients, and oxygen to metabolically active zones (Gooseff et al. 2004; Covino et al. 2010b, 2011; Knapp et al. 2017; Gootman et al. 2020). The extent of water exchange controls the residence time of solutes (Drummond et al., 2012; Gomez et al., 2012; Patil et al., 2013), their chemical signatures (Covino and McGlynn 2007), as well as the microbial composition and their metabolic functioning (Blume et al. 2002; Navel et al. 2011; Li et al. 2020). Exchange patterns are influenced by geomorphologic conditions (Kasahara and Wondzell 2003; Cardenas et al. 2004; Gooseff et al. 2005; Emanuelson et al. 2022), hydrologic conditions (i.e., discharge and surrounding water table configuration) (Gooseff et al. 2005; Wondzell 2006; Ward et al. 2013; Ward and Packman 2019), and even biofilm growth (Battin et al. 2003; Wen and Li 2018). The spatiotemporal variability in exchange processes and resource availability (e.g., seasonal variations in nutrient loads) create heterogeneous hydrologic and biogeochemical gradients across space and time, within which ecosystem metabolism occurs (Mulholland et al., 1985; Mulholland & Hill, 1997).

To date, studies with a focus on hydrologic transport argue that longer residence times across a stream ecosystem should consistently result in higher biological demand for carbon, nutrients, and oxygen (Valett et al. 1996; Gooseff et al. 2005; Wondzell 2006; Gomez et al. 2012; Zarnetske et al. 2012; Ward et al. 2013; Li et al. 2021), not fully incorporating the potential for biologically mediated reactions to be limited by stoichiometric imbalances. Ecological stoichiometry is the notion that biota balances the consumption of nutrients with energy requirements. Redfield (1934) noted that marine phytoplankton generally contained a ratio of C:N:P of 106:16:1 in their biomass, and these ratios are similar to those available in their environment. This “Redfield ratio” suggests that an ecosystem requires an optimal distribution of available nutrients to flourish and has been used as a guide for many other environmental stoichiometry studies. In a study of streams across eight biomes, Dodds et al. (2004) noted that N retention depends in part on the C:N ratio of organic matter in streams and suggested that shifts in these state ratios likely influence N retention.

The net effect of supply and demand of resources can be explored with the non-dimensional Damköhler number, *Da* (Harvey et al. 2013; Pinay et al. 2015; Krause et al. 2017; Ocampo et al. 2020), which quantifies the ratio of transport (i.e., supply) to biological uptake (i.e., demand) timescales along flow paths (Oldham et al. 2013; Liu et al. 2022). Similar to any other non-dimensional number, *Da* offers simplicity and objectivity for inter-site and intra-site comparisons. *Da* has been used to provide insight into the factors limiting the supply and demand of resources (Harvey et al. 2005), as values of *Da*~ 1 define a balance between transport and uptake time scales, which theoretically result in maximal resource retention. Accordingly, where or when $Da << 1$, i.e., the uptake timescale is much greater than the transport timescale, uptake is suboptimal, and it is referred to as reaction limited because even though resources became available through hydrologic exchange, they were not fully taken up (i.e., assimilated). Conversely, where or when $Da >> 1$, i.e., the transport timescale is much greater than the uptake timescale, resources become scarce or transport-limited, and biologically inactive subregions start to develop (González-Pinzón and Haggerty 2013; Harvey et al. 2013; Gootman et al. 2020). While *Da* captures essential components of the potential interactions between the supply and demand of ecologically relevant resources, it does not explicitly capture the role

https://doi.org/10.5194/bg-2022-214
Preprint. Discussion started: 9 November 2022

of stoichiometric limitations on the supply (i.e., C:N:P ratios in water fluxes) and demand (C:N:P biomass composition and needs) of resources. This is mainly because *Da* numbers are estimated from solute-specific mass balances, which inform transport and reaction timescales for one resource at a time (e.g., only N), in isolation of other stoichiometrically relevant resources that can become limiting factors (e.g., C and P).

Based on the relevance and co-dependences between hydrologic exchange, stoichiometry, and biological uptake, and the limited amount of field studies available to determine their net effects on the retention and export of resources, we sought to quantify how metabolic activity is controlled by the interactions and supply of essential nutrients (C, N, P). More specifically, we tested if variations in stoichiometric conditions can induce metabolic limitations at which residence time alone becomes a weak predictor of stream respiration. We addressed the following research question: *How is microbial respiration controlled by hydrologic exchange vs. stoichiometric conditions (i.e., supply of C, N, and P)*? We hypothesized that aerobic respiration would be maximized when nutrient supply and demand were nearly balanced for a given hydrologic condition. To test this, we conducted a repeated set of stream tracer injections in Como Creek, a mountain stream in Colorado, USA, varying stream C (acetate; sensu Baker et al., 1999), N ($NaNO_3$), and P (KH_2PO_4) concentrations to manipulate stoichiometry and nutrient supply. We repeated experiments under different flow conditions to quantify the tradeoffs between supply (transport and delivery of nutrients), and demand (microbial respiration). We tested for statistical relationships between hydrologic transport metrics and respiration metrics using the resazurin-resorufin tracer system (González-Pinzón et al., 2012; Knapp et al., 2018) and contextualized our findings within the framework of the Damköhler number.

2 Methods

2.1 Site Description

Our research experiments were conducted in Como Creek, a forested pool and riffle stream in Colorado, USA. Como Creek is a tributary to Boulder Creek, with land cover consisting of approximately 20% alpine meadow-tundra and 80% conifer forest. The study reach drains a 5.4 km^2 catchment, with elevations ranging from 2895-3557 m and a mean average precipitation of 883 mm/y (Ries III et al. 2017; Emanuelson et al. 2022). Como Creek has a snowmelt-driven hydrograph with stream discharges ranging from 1-98 L/s and features short-lived increases in discharge during the monsoon season between July and August (Figure 1). The study reach is a multi-thread channel with substrate ranging from small gravel to bedrock. Additionally, the channel has an average width-to-depth ratio of 11.5, a sinuosity of 1.1, and an average longitudinal slope of 21% (Natural Resources Conservation Service).

https://doi.org/10.5194/bg-2022-214
Preprint. Discussion started: 9 November 2022

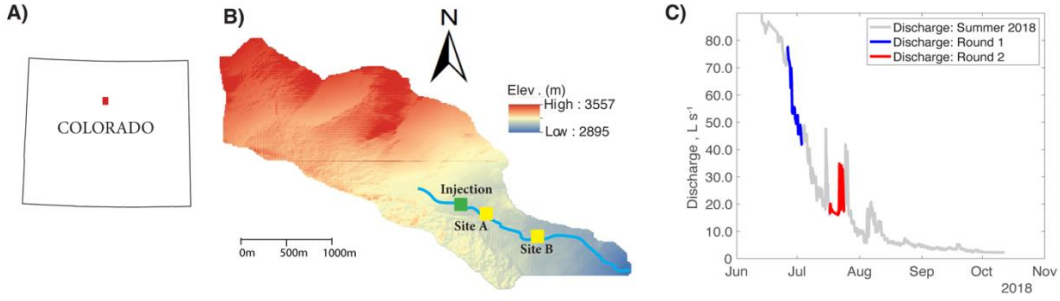

Figure 1. A) Location of Como Creek watershed in Colorado, B) detailed map of the watershed where Sites A and B are 50 and 350 m downstream from the injection location, and C) hydrograph and timing of experimental work; each round of experiments consisted of four treatments featuring N, N+C, N+P, and C+N+P nutrient additions.

2.2 Stream tracer injection experiments

We conducted two rounds of experiments, each consisting of four sets of continuous injections (lasting ~ 4-7 h) of Cl^- as a conservative tracer, resazurin (referred to as Raz hereafter) as a proxy for aerobic respiration, and one of the following nutrient treatments: a) N, b) N+C, c) N+P, and d) C+N+P. In our study, the nutrient treatments are treated as known system modifications (control variables) to alter metabolism. Also, we use the transformation of Raz, which occurred at the same spatiotemporal scales of the nutrient additions, to calculate how changes in stoichiometric conditions and discharge affect respiration. Briefly, the reactive tracer Raz (blue in color) is irreversibly reduced to resorufin (Rru, red) under aerobic respiration, and the relationship between Raz transformation and oxygen consumption is linear (González-Pinzón et al. 2012, 2014, 2016; Knapp et al. 2018; Dallan et al. 2020). Table 1 shows the masses injected and the discharges observed during the studies. Note that we allowed the stream to return to ambient concentrations for one day after each set of injections.

Table 1. Tracer injection data for each round of experiments at Como Creek.

Date	Treatment	Discharge (L/s)	Start time	End time	NaCl (g)	KNO_3 (g)	KPO_4 (g)	Sodium Acetate (g)	Raz (g)
Round 1									
6/26/18	N	74	11:30	17:00	32653	502	-	-	150
6/28/18	N+C	61	10:08	14:10	32680	500	-	2000	150
6/30/18	N+P	53	10:00	17:00	32680	500	400	N/A	150
7/2/18	C+N+P	49	9:59	14:00	32680	500	400	2000	150
Round 2									
7/17/18	N	20	10:30	14:35	10000	100	-	-	30
7/19/18	N+C	17	10:00	13:59	10000	100	-	400	30
7/21/18	N+P	17	10:00	14:06	10000	100	80	-	30
7/23/18	C+N+P	25	9:30	13:35	10000	100	80	400	30

https://doi.org/10.5194/bg-2022-214
Preprint. Discussion started: 9 November 2022


Biogeosciences Discussions Open Access EGU

We collected 20 mL aliquots in each tracer injection 50m and 350m downstream of the injection site (labeled Sites A and B, Figure 1) to generate tracer breakthrough curves (BTCs) for Raz. All samples were filtered immediately after being collected using a 0.7 µm GF/F filter (Sigma-Aldrich) and kept on dry ice during transport until they were frozen at -4ºC for laboratory analysis for Raz concentrations. All analyses took place within a week after the end of each round of injections. At the laboratory, each sample was buffered to a pH of 8.5 (1:10 buffer-to-sample) following Knapp et al. (2018). The fluorescence signals were measured with a Cary Eclipse Fluorescence Spectrophotometer (Agilent Technologies) using excitation/emission wavelengths of 602/632 nm for Raz and 571/584 nm for Rru and converted to concentrations based on an 8-point calibration curve (R^2=0.99).

2.2 Conservative transport modelling and metrics

We calibrated the conservative transport parameters of the transient storage model presented in Equations 1 and 2 using Cl^- and streamwater electrical conductivity data observed at Sites A and B. For this, we used the Matlab (The Mathworks Inc., Natick, Massachusetts) script from Knapp et al. (2018), which features a joint calibration of conservative and reactive solutes through a non-linear, least squares optimization routine.

$$\frac{\partial c}{\partial t} = -u\frac{\partial c}{\partial x} + D\frac{\partial^2 c}{\partial x^2} - \frac{A_s}{A}\frac{\partial c_{ts}}{\partial t} + q_{in}c - \lambda_{mc}c \quad (1)$$

$$\frac{\partial c_{ts}}{\partial t} = k(c - c_{ts}) - \lambda_{ts}c_{ts} \quad (2)$$

where c [ML^{-3}] and, c_{ts} [ML^{-3}] are the concentrations in the main channel and aggregate transient storage zone; x [L] is the distance of the study reach; t [T] is time; u [LT^{-1}] and D [L^2T^{-1}] are parameters representing advective flow velocity and dispersion coefficient, respectively; q_{in} [T^{-1}] is a volumetric flux parameter accounting for lateral inputs; $k[T^{-1}]$ is the first-order mass transfer rate coefficient parameter between the main channel and the aggregate transient storage zone; A_s/A $[-]$ is the capacity ratio parameter representing the relative contribution of transient storage-dominated to advection-dominated compartments in the stream, represented as areas along the reach; and λ_{mc} and λ_{mc} [T^{-1}] are processing-rate coefficients in the main channel and transient storage zones (equaling zero for a conservative tracer).

We estimated conservative transport timescales from the transport parameters to describe the transient storage timescale, $\tau_{sz} = 1/k$ [T], and the mean travel time between sites A and B, τ [T], which was computed as:

$$\tau = \frac{m_{1,cl}}{m_{0,cl}} \quad (3)$$

$$m_n = \sum_{i=1}^{r}\left(\frac{t_i + t_{i+1}}{2}\right)^n \left(\frac{C_i + C_{i+1}}{2}\right)(t_{i+1} - t_i) \quad (4)$$

where $m_{0,cl}$ and $m_{1,cl}$ are the zeroth and first-centralized temporal moments of the Cl^- BTCs from each sampling site, i is a time index, r is the total number of samples available in a BTC.

https://doi.org/10.5194/bg-2022-214
Preprint. Discussion started: 9 November 2022

2.3 Estimating the transformation of Raz as a proxy for microbial respiration:

We used the net transformation rate coefficients of Raz, λ_{Raz} [T^{-1}], as a proxy for microbial respiration (González-Pinzón et al. 2012, 2014, 2016; Knapp et al. 2018; Dallan et al. 2020), and estimated them following the work by González-Pinzón and Haggerty (2013), which derived algebraic relationships to calculate processing rate coefficients from the transient storage model presented here in Equations 1 and 2:

$$\lambda_{Raz} = \lambda_{mc_{Raz}} + \lambda_{ts_{Raz}} = \frac{\ln\left(m^{inj}_{0,Raz}/m^{BTC}_{0,Raz}\right)}{\tau}\left(1 + \frac{\overbrace{\ln\left(m^{inj}_{0,Raz}/m^{BTC}_{0,Raz}\right)}^{dispersion\ term,\Phi}}{Pe}\right) \quad (5)$$

where $m^{inj}_{0,Raz} = M_{Raz}/Q$ is the zeroth temporal moment of Raz at the injection site [M L^{-3} T^{-1}], M_{Raz} is the mass of Raz added to the injectate, Q is the stream discharge [L^3T^{-1}]; $m^{BTC}_{0,Raz}$ is the dilution-corrected zeroth temporal moment of Raz estimated with BTC data from a sampling site; and $Pe = L\,u/D$ is the Peclet number [-], which describes the relative importance of advection and dispersion in the system. In the work by González-Pinzón and Haggerty (2013), the use of zeroth temporal moments implied that only one processing-rate coefficient could be estimated from every observed BTC available. However, using the conceptual principles proposed in the Tracer Addition for Spiraling Curve Characterization (TASCC) framework (Covino et al. 2010b), multiple rate coefficients can be estimated from an equivalent version of Equation 5.

Briefly, TASCC uses the dynamic range of solute concentrations sampled in BTCs to characterize uptake kinetics from ambient to saturation concentrations. In TASCC, the ratio of reactive to conservative solute concentrations for every independent sample across the tracer BTCs is compared to the ratio of the concentrations of the injection solution to determine uptake metrics. If the added solutes are non-limiting or non-reactive, they will transport conservatively, and the ratio of the reactive to conservative solute concentrations will remain constant. Alternatively, if the added solutes are limiting, co-limiting or reactive, they will not transport conservatively, and the ratio of the reactive to conservative solute concentrations will change over time as a function of reactivity.

To incorporate the TASCC framework into the algebraic equation developed by González-Pinzón and Haggerty (2013) and estimate transformation rate coefficients for Raz from each pair of conservative (i.e., $C_{cons.}$) and reactive tracer concentrations (i.e., C_{Raz}), we need to replace m_0 with $C_{Raz}/C_{cons.}$ This guarantees that the mean value of all the processing-rate coefficients is equal to the processing-rate coefficient estimated from the zeroth temporal moment analysis of model-derived simulations from Equations (1) and (2). Accordingly:

$$\lambda_{Raz,sample} = \frac{\ln\left[\frac{C_{Raz}}{C_{cons.}}\right]_{inj} - \ln\left[\frac{C_{Raz}}{C_{cons.}}\right]_{BTC}}{\tau}\left(1 + \frac{\overbrace{\ln\left[\frac{C_{Raz}}{C_{cons.}}\right]_{inj} - \ln\left[\frac{C_{Raz}}{C_{cons.}}\right]_{BTC}}^{dispersion\ term,\Phi}}{Pe}\right). \quad (6)$$

https://doi.org/10.5194/bg-2022-214
Preprint. Discussion started: 9 November 2022


Biogeosciences Discussions Open Access EGU

Equation 6 directly links different transport mechanisms used to explain the transport and fate of solutes (i.e., advection, dispersion, transient storage, and reactivity) with TASCC, an algorithm yielding higher information content from experimental work. We note here that alternative forms of Equation 6 can be derived for solute transport models, including additional reactions such as sorption and production. Therefore, similar new equations could be derived to provide mechanistic explanations to TASCC-related findings noticing hysteresis behavior in nutrient uptake between the rising and falling limbs of experimental BTCs (Gibson et al. 2015; Trentman et al. 2015; Rodríguez-Cardona et al. 2016; Brooks et al. 2017; Day and Hall 2017).

Finally, from each transformation rate coefficient $\lambda_{Raz,\ sample}$, we also estimated an uptake (or mass transfer) velocity of Raz, $V_{f_{Raz,sample}} = \lambda_{Raz,sample} \cdot h$, where h is the mean depth of the stream. Following Ensign and Doyle (2006), uptake velocities represent the vertical velocity of solute molecules through the water column towards the benthos and are typically used in stream ecology to normalize processing-rate coefficients by the influence from contrasting discharge magnitudes to facilitate the comparison of results from small streams and large rivers.

2.4 Statistical tests

We calculated standard deviations (std) based on repeated measures of the distribution of the transport parameters of Equations 1 and 2 to create upper and lower boundaries of the uncertainties in our measurements (i.e., mean ± std). Because our data were not normally distributed, we used the Mann-Whitney U nonparametric statistical test to determine if there were statistically significant differences between nutrient treatments across rounds (e.g., N vs. N in rounds 1 and 2), following a similar procedure in Ensign and Doyle (2006). For the Mann-Whitney U test, we set our significance level (α, alpha) equal to 0.05.

We explored the Pearson correlation coefficient (r) matrix between the transport parameters of Equations 1 and 2, and associated metrics, to establish direct (r >0.1), inverse (r <-0.1), and non-existent correlations (-0.1< r <0.1) (Bowley 2008). We classified the strength of the correlations as uncorrelated (0< r <|0.1|), weakly correlated (|0.1|< r <|0.5|), moderately correlated (|0.5|< r <|0.8|), strongly correlated (|0.8|< r <|1.0|), and included p-values for each correlation.

Lastly, we tested differences in mean values of the transport parameters of Equations 1 and 2, and associated metrics, between nutrient treatments within each experimental round (e.g., N vs. N+C vs. N+P vs. C+N+P in round 1) using the Student's *t*-test based on deviation from the group's mean value (Blair et al. 1980).

3 Results and Discussion

3.1 Conservative transport and metrics of physical controls

Between experimental rounds 1 and 2, stream depth (h) and discharge (Q) decreased, causing significant differences in stream velocity (u), dispersion (D), mass-transfer rate coefficients (k), transient storage time scales

https://doi.org/10.5194/bg-2022-214
Preprint. Discussion started: 9 November 2022

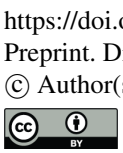

(τ_{TS}) and mean travel times (τ) (Figure 2). The only parameter that did not show significant differences was the relative contribution of the main channel to storage zone areas, A_s/A.

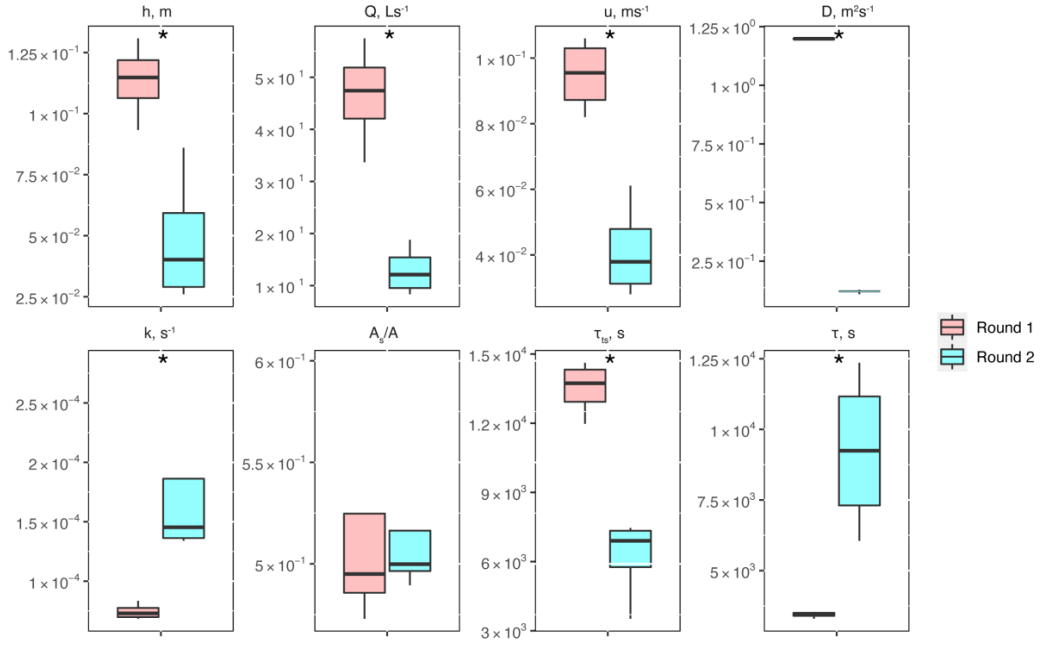

Figure 2. Conservative transport parameters and metrics of physical controls estimated for the two experimental rounds: stream depth (h), stream velocity (u), dispersion (D), mass transfer rate coefficients (k), the ratio of transient storage-dominated to advection-dominated compartments (A_s/A), transient storage time scales (τ_{TS}) and mean travel times (τ). Asterisks represent statistical differences in magnitudes for rounds 1 and 2 with p<0.05 (*) based on the Mann-Whitney U nonparametric statistical test.

The correlation matrix between parameters and metrics (Figure 3) shows that Q (and interrelated quantities h and u), D, and τ_{ts} were all directly correlated (from moderately to strongly). Mean travel times between sites, τ, were directly and weakly correlated with k and the ratio A_s/A, and inversely correlated (from weakly to strongly) with the rest of the conservative transport parameters and metrics. Finally, the ratio A_s/A was generally uncorrelated or weakly correlated with other quantities. Even though the correlations of some interdependent quantities are known to be spurious, e.g., Q vs. u and λ_{Raz} vs. $V_{f_{Raz}}$ (González-Pinzón et al. 2015), we included all relevant measured and modeled quantities in Figure 3 to allow readers to explore different data pairs. For clarity, we differentiate with brackets all known spurious correlations. Note that we did not flag the correlation between A_s/A and Q (and their interrelated quantities h and u) as spurious because the ratio of areas is an indicator of the relative volume-based contribution from advection-dominated to transient storage-dominated compartments, instead of actual estimates of cross-sectional areas (Kelleher et al. 2013; González-Pinzón et al. 2013; Knapp and Kelleher 2020).

https://doi.org/10.5194/bg-2022-214
Preprint. Discussion started: 9 November 2022

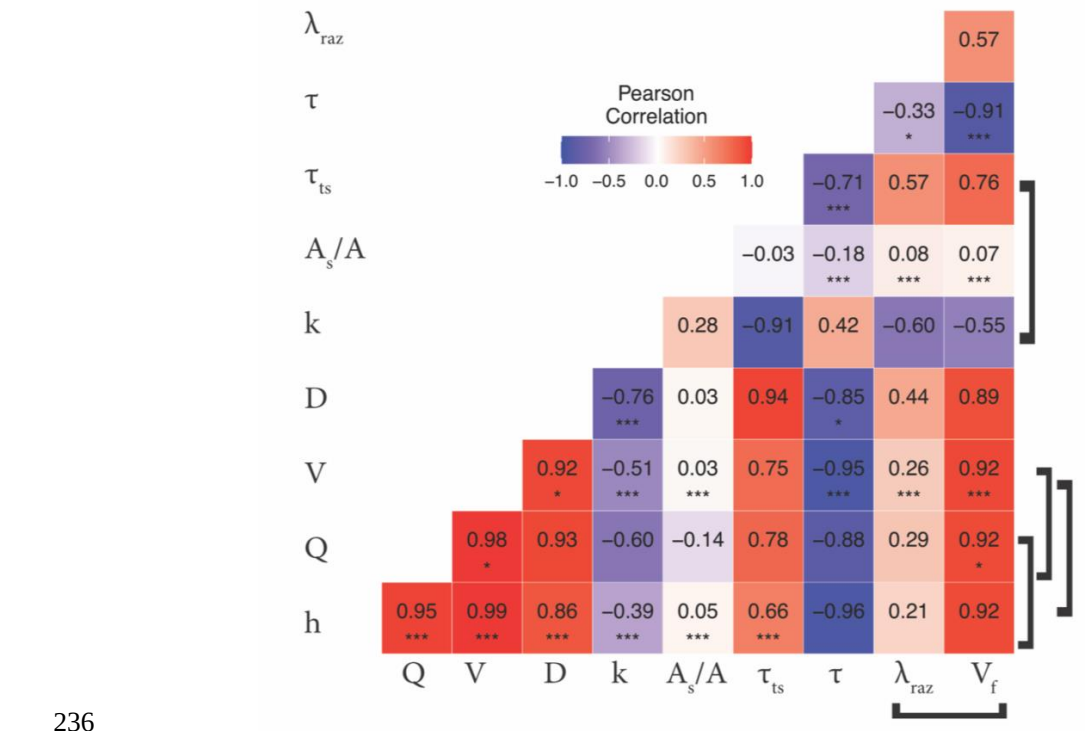

Figure 3. Pearson correlation coefficient (r) heatmap for the mean values of the transport parameters and metrics for each stoichiometric treatment during rounds 1 and 2. Brackets link known spurious correlations. Asterisks represent significant differences in magnitudes between parameters with p<0.05 (*), and p<0.001(***) based on the Pearson Correlation.

One of the metrics of interest in stream reactive-transport modeling is the transient storage timescale ($\tau_{ts} = 1/k$), which quantifies the exposure that solutes have to biological communities in metabolically active transient storage zones. In our study site, τ_{ts} decreased one order of magnitude from round 1 to round 2, and were comparable to the range of values observed in other studies involving forested mountain streams (Valett et al. 1996; Hall et al. 2002). Due to the geomorphology of the stream, which is characterized by steep longitudinal and valley slopes, pool and riffle sequences, and shallow bedrock, transient storage was expected to occur mainly in the main channel (Fields and Dethier 2019; Barnhart et al. 2021; Emanuelson et al. 2022). As flow receded from round 1 to round 2, we observed the disconnection of in-stream pools contributing to transient storage, which explains the direct correlation between discharge and transient storage timescales. Another indication of the dominant contribution of in-stream pools to total transient storage is the lack of change of A_s/A with discharge, which suggests that the contribution of transient storage-dominated (i.e., A_s) and advection-dominated compartments (i.e., A) varied proportionally over changes in discharge.

https://doi.org/10.5194/bg-2022-214
Preprint. Discussion started: 9 November 2022

3.2 Raz transformation (a proxy for respiration) as a function of physical controls

Our results indicate that the transformation of Raz (λ_{Raz}) was directly and moderately correlated with the transient storage timescale (τ_{ts}), as other studies on reactive transport have shown (Valett et al. 1996; Hall et al. 2002; Gomez et al. 2012; Zarnetske et al. 2012; Kiel and Bayani Cardenas 2014; Gootman et al. 2020). The mean values of λ_{Raz} were directly and weakly correlated with discharge (Q) (also depths h and velocities u) and dispersion (D), and directly and moderately correlated with τ_{ts}. The transformation rate coefficient of Raz (λ_{Raz}) values were inversely and weakly correlated with mean travel times (τ), and inversely and moderately correlated with mass-transfer rate coefficients (k) (Figure 3). Raz uptake velocities ($V_{f_{Raz}}$) showed spurious, direct and strong correlations with discharge (Q) (also h and u), strong correlations with dispersion (D) and transient storage timescales (τ_{ts}), and strong indirect correlations with mean travel times (τ) and k (moderate). Finally, both λ_{Raz} and $V_{f_{Raz}}$ were uncorrelated with A_s/A. Unlike studies where an increased transient storage timescale (τ_{ts}) is mainly associated with slower hyporheic flows due to lower discharges (Q) (Zarnetske et al. 2007; Schmid et al. 2010), τ_{ts} in our study site increased with Q because the geomorphology of the channel and the valley favored in-stream transient storage in pools (Jackson et al. 2012, 2013, 2015), and the metabolically active biofilms available there may have prompted the transformation of Raz (Haggerty et al. 2014; Peralta-Maraver et al. 2018). Consistently, when stream flows recede in these types of streams, the subsequent disconnection of parts of the channel causes a decline in transient storage and metabolism (Covino et al. 2010a; Emanuelson et al. 2022). Hall et al. (2002) found similar results in a study of thirteen streams, where changes in stream width and depth primarily drove variations in transient storage timescales.

3.3 Raz transformation (a proxy for respiration) as a function of physical and stoichiometric controls

Our results suggest no significant changes in respiration despite significant differences in discharge (Q) and nutrient treatments. Between experimental rounds, the mean values of Q (and h and u by extension) were statistically different for each treatment comparison (Figure 4A). For λ_{Raz}, we only found statistical differences between rounds for the C+N+P treatments (Figure 4B). Due to the large influence of Q on the uptake velocity of Raz ($V_{f_{Raz}}$) through stream depth (h), the statistical differences between rounds seen for Q were also seen for $V_{f_{Raz}}$ (Figure 4C).

https://doi.org/10.5194/bg-2022-214
Preprint. Discussion started: 9 November 2022

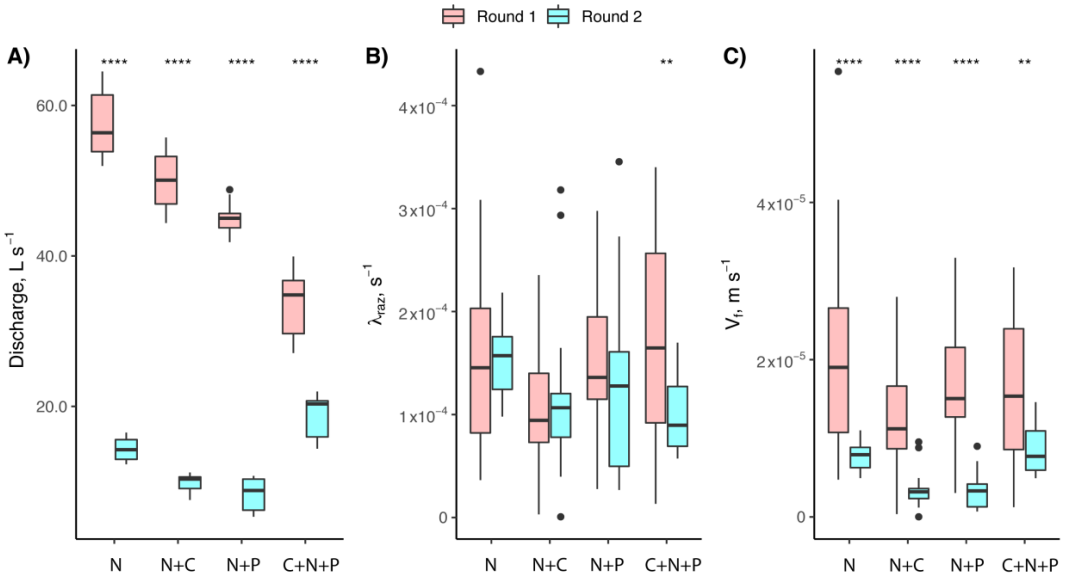

Figure 4. Comparison of A) stream discharge values recorded at the gaging station, B) transformation rate coefficients of resazurin (λ_{Raz}) resulting from Equation 6, and associated C) uptake velocities of resazurin ($V_{f_{Raz}} = \lambda_{Raz}\, h$) estimated for each experimental nutrient treatment addition during rounds 1 and 2. Due to the large influence of Q on the uptake velocity of Raz ($V_{f_{Raz}}$) through stream depth (h), most of the statistical differences between rounds seen for Q were also seen for $V_{f_{Raz}}$. Asterisks represent significant differences in magnitudes between rounds with p<0.01(**), and p~0 (****) based on the Mann-Whitney U nonparametric statistical test.

When looking at the data collected from each round, we found that mean Q values were statistically different across nutrient treatments (Figures 5A and 5D). For mean λ_{Raz} values, the only treatments with statistical differences were the N+C and C+N+P from round 1 (Figures 5B and 5E). Finally, $V_{f_{Raz}}$ mean values were only statistically different for the N vs N+C treatments for round 1, and for all but the N+C vs N+P and N vs C+N+P treatments for round 2 (Figures 5C and 5F).

https://doi.org/10.5194/bg-2022-214
Preprint. Discussion started: 9 November 2022

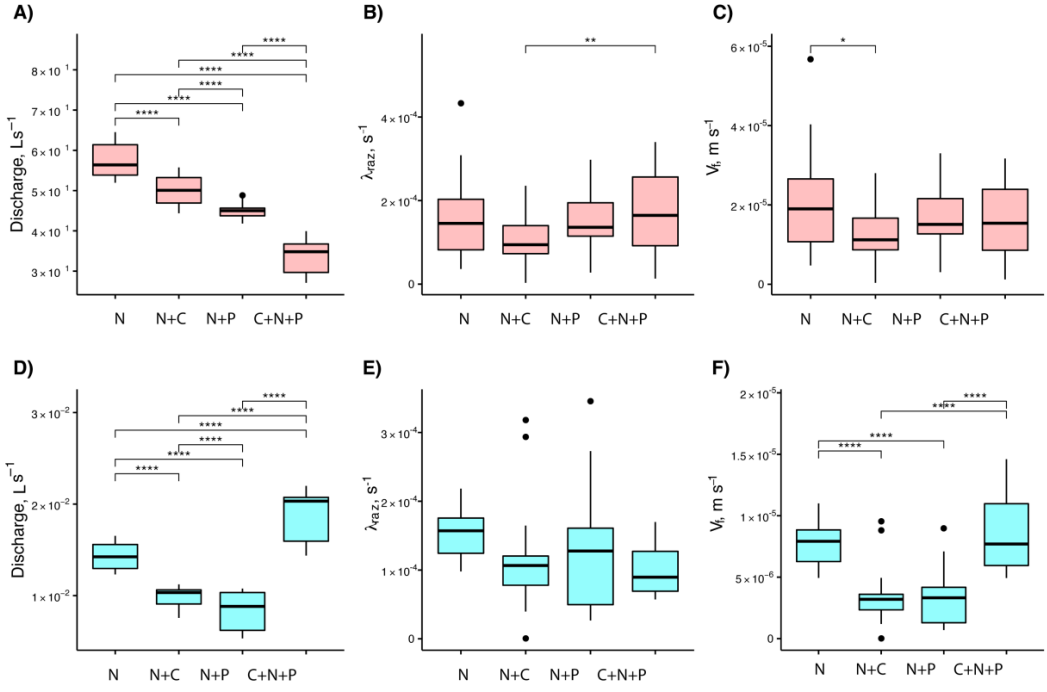

Figure 5. Comparison of stream discharges (A and D), transformation rate coefficients of resazurin (λ_{Raz}) (B and E), and uptake velocities of resazurin ($V_{f_{Raz}}$) (C and F) across treatments for round 1(top row) and 2 (bottom row). Due to the large influence of Q on the uptake velocity of Raz ($V_{f_{Raz}}$) through stream depth (h), most of the statistical differences between rounds seen for Q were also seen for $V_{f_{Raz}}$. Asterisks represent significant differences in magnitudes for treatments N, N+C, N+P, and C+N+P with p<0.05 (*), p<0.01(**), and p~0 (****) based on the Mann-Whitney U nonparametric statistical test.

For each of the eight nutrient injections, we related the mean transient storage timescales, τ_{ts}, which indicate exposure times between solutes and microbial communities, and the mean transformation timescales of Raz, $1/\lambda_{Raz}$, which indicate respiration (Figure 6). This Damköhler-based analysis allows us to visualize the interplay between physical, biological, and stoichiometric controls in the stream. We found that the range of variation of the mean transient storage timescales was three times greater than that of the mean transformation timescales. This suggests that the changes brought by our stoichiometric controls (color-coded in Figure 6) may have contributed to buffer changes in microbial respiration. In round 1, all the stoichiometric treatments resulted in transport-limited conditions, i.e., the average particle of Raz that entered a metabolically active compartment underwent transformation and more Raz could have been transformed if it had been available. Thus, in round 1, respiration was high relative to the supply of solutes to the metabolically active transient storage zones. In round 2, all stoichiometric treatments, except N, resulted in reaction-limited conditions, i.e., the average particle of Raz entering a metabolically active compartment left it without undergoing transformation. Thus, in round 2, respiration was slow relative to the exposure of solutes to microbial communities.

https://doi.org/10.5194/bg-2022-214
Preprint. Discussion started: 9 November 2022

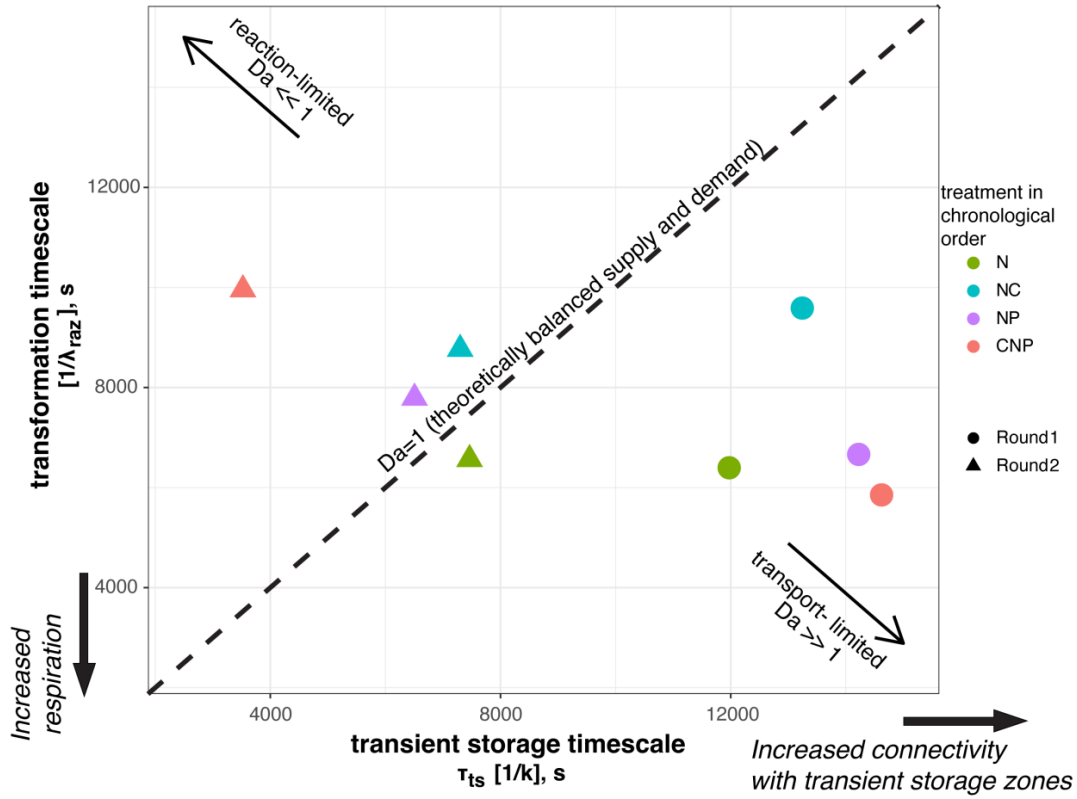

Figure 6. Mean reaction and transient storage timescales for each nutrient treatment. The Damköhler, Da = transient storage timescale/ transformation timescale, indicates reaction-limited and transport-limited conditions.

3.4 How is microbial respiration controlled by hydrologic exchange vs. stoichiometric conditions (i.e., supply of C, N, and P)?

We characterized microbial respiration with the transformation timescale of Raz, $1/\lambda_{Raz}$; the extent of hydrologic exchanges with the transient storage timescale, τ_{TS}, and the relative size of the main channel and transient storage areas, A_s/A; and stoichiometric conditions with our controlled nutrient additions (i.e., N, N+C, N+P, and C+N+P treatments). The most salient findings indicate that a) discharge (Q) changed significantly between rounds (Figure 4a) and across stoichiometric treatments (Figure 5a, 5d), and was directly and moderately correlated with τ_{TS} and uncorrelated with A_s/A (Figure 3), suggesting that most transient storage occurred in the side pools in the channel, which increased in quantity and extent proportionally with Q, and b) the respiration activity indicated by λ_{Raz} remained similar between rounds with significantly different Q (Figure 4b), and across controlled stoichiometric treatments also featuring different Q (Figure 5b, 5e). Thus, we observed that respiration remained largely unchanged or constant with varying physical and stoichiometric conditions, as we summarized in Figure 7.

https://doi.org/10.5194/bg-2022-214
Preprint. Discussion started: 9 November 2022

Given that each experimental round lasted only one week, in the absence of stoichiometric manipulations, we would have expected to see changes in microbial respiration proportional to the constraints imposed by the physical controls in the stream. This expectation is based on the assumption that there are insignificant changes to the microbial composition of a stream during any given week. Consequently, the disconnection of surface transient-storage zones with microbial biomass due to the marked flow recessions should have resulted in reduced transformation of Raz, i.e., reduced respiration (González-Pinzón et al. 2012, 2014; Knapp et al. 2017, 2018). Within this context, the constant respiration that we observed in our study may have resulted from counterbalanced interactions between flow reductions, which decreased surface transient storage and the amount of biomass connected to the stream, and an increase in metabolic activity likely prompted by the removal of nutrient limitations from our sequential additions of N, N+C, N+P, and C+N+P (Figure 7). This is supported by evidence showing that microbial biofilms operate as rate-limited systems, where solutes and particulates can remain stored longer and be utilized later than the resources transported in the main channel (Battin et al. 2003, 2016; Merchant and Helmann 2012). Therefore, even if our nutrient additions were carried out every other day to allow the stream to return to ambient conditions, nutrients might have become increasingly more abundant inside connected biofilms, progressively contributing to reducing nutrient limitations. Simply put, while less biomass contributed to respiration when side pools became disconnected through flow reductions, the connected biofilms may have been more metabolically active, causing constant respiration activities.

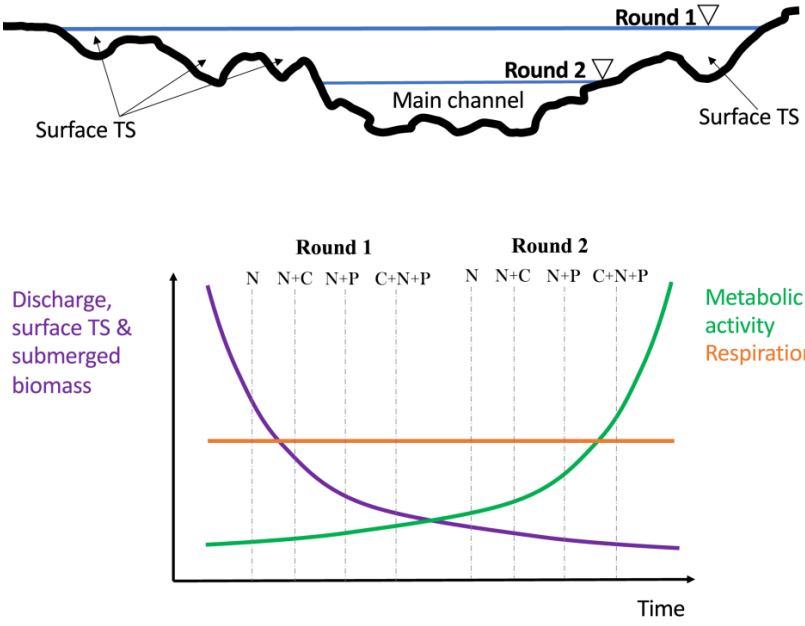

Figure 7. Conceptual diagram explaining constant stream respiration in Como Creek: the study featured flow recession and two rounds of stoichiometric treatments: N, N+C, N+P, and C+N+P.

https://doi.org/10.5194/bg-2022-214
Preprint. Discussion started: 9 November 2022


Biogeosciences Discussions Open Access EGU

Our findings support the idea that transient storage timescales alone could be a weak predictor of stream respiration due to the relevance of local and dynamic variations in stoichiometric conditions. In previous studies, transient storage and nutrient uptake have presented contradictory relationships:

Inconclusive relationships: Martí et al. (1997) did not find correlations between NH_3 uptake length and A_s/A in a desert stream using data from eight tracer injections. Webster et al. (2003) did not find statistically significant relationships between NH_4 uptake and A_s/A using the 11-stream LINX-I dataset that included arctic to tropical streams. From thirty seven injections conducted in thirteen streams at Hubbard Brook Experimental Forest (HBEF), Hall et al. (2002) found weak correlations (R^2=0.14-0.35) between transient storage parameters and NH_4 demand. Using data from seven streams in New Zealand, Niyogi et al. (2004) did not find significant correlations between soluble reactive phosphorous (P-SRP), NO_3 uptake velocities, and A_s/A. Bukaveckas (2007) reported an indefinite relationship between transient storage and NO_3 and P-SRP retention efficiencies from tracer injections in a reference (N=13 injections), a channelized (N=14 injections), and a restored (N=17 injections) stream reach in the midwestern US. Lastly, the LINX-II dataset from ^{15}N-NO_3 injections in 72 streams located in eight regions of the US showed no relationship between NO_3 uptake and the fraction of median travel time due to transient storage (F_{med}^{200}) (Hall et al. 2009).

Weak to moderate relationships: Thomas et al. (2003) showed that transient storage accounted for 44% to 49% of NO_3 retention measured by ^{15}N in a small headwater stream in North Carolina. Mulholland et al. (1997) found larger PO_4 uptake rates in a stream with higher transient storage, when they compared two forested streams. Ensign and Doyle (2005) found an increase in A_s/A and the uptake velocities for NH_4 and PO_4 after the addition of flow baffles to two streams. Lautz and Siegel (2007) found a modest correlation (R^2=0.44) between NO_3 retention efficiency and transient storage in the Red Canyon Creek watershed, WY.

Strong relationships: Valett et al. (1996) found a strong correlation (R^2=0.77) between transient storage and NO_3 retention in three first-order streams in New Mexico. From nine tracer injections in two urban streams in the eastern US, Ryan et al. (2007) found strong relationships between P-SRP retention and transient storage metrics ($k, A_s/A$; R^2>0.84) when the variables were measured in different seasons. Sheibley et al. (2014) observed that the retention of NO_3 in seven agricultural streams in the US was positively correlated with A_s/A and the average water flux through the storage zone per unit length of stream ($q_s = kA$), and negatively correlated with the transient storage timescale (τ_{ts}). However, they found no significant correlation between NH_4^+ and SRP retention and transient storage metrics.

The studies referenced above were done in streams with contrasting physical, chemical, and biological conditions. Together, they offer a broader perspective on the inconsistent relationship between transient storage metrics and metabolic processing. Those studies do not feature co-injections of C, N, and P macronutrients (e.g., N+C, N+P, N+C+P), even while some tracked ambient processing rates of more than one nutrient. Therefore, they generally represent solute-specific analyses, where the uptake of one nutrient at a time was analyzed and, thus, did not account for stoichiometric controls on nutrient uptake. On the contrary, our study offers evidence suggesting that stoichiometric controls can be as important as physical controls in establishing reach-scale metabolic activities, explaining why transient storage timescales alone could be a weak predictor of stream metabolic processes.

https://doi.org/10.5194/bg-2022-214
Preprint. Discussion started: 9 November 2022

4 Conclusions

We conducted two rounds of four stoichiometric treatments (i.e., N, C+N, N+P, and C+N+P) in a headwater stream in Colorado to quantify changes to stream respiration during flow recession and answer the question: *How is respiration controlled by hydrologic exchange vs. stoichiometric conditions (i.e., supply of C, N, and P)*? We found that discharge changed significantly between rounds and across stoichiometric treatments, and that it was directly and moderately correlated with transient storage timescales but uncorrelated with the ratio of contributions from advection-dominated to transient storage-dominated compartments (i.e., A_S/A). This suggests that most transient storage occurred in side pools within the main channel, which increased in quantity and extent proportionally with discharge. We also found that respiration remained similar despite significant changes in discharge and stoichiometric treatments. Our results contradict the notion that hydrologic transport alone is a dominant control on biogeochemical processing, as longer transient storage timescales were not uniquely associated with increased respiration in our study. Interestingly, our results suggest that the sequential stoichiometric treatments that we conducted over the two rounds of experiments counterbalanced the controls imposed by hydrologic transport, consistently resulting in insignificant changes in stream respiration between rounds and treatments. Together, we saw that residence time alone could be a weak predictor of stream respiration due to the relevance of local and dynamic variations in stoichiometric conditions. Our results offer a plausible explanation for the lack of consistency in reported relationships between transient storage and in-stream nutrient processing from prior studies.

Author contribution: RGP, TC, KS, and MG secured the funding for this research. All co-authors designed carried out the experiments. JD and RGP processed Raz/Rru samples, performed solute transport simulations, statistical analyses, and prepared the manuscript with input from all co-authors. All co-authors approved the final version of the manuscript.

Acknowledgments

The National Science Foundation provided funding support through grants NSF EAR-1642399, NSF EAR-1642368, NSF EAR-1642402, and NSF EAR-1642403. We thank Karin Emanuelson, Jackie Randell, Erin Jenkins, Tristan Weiss, and Melissa Pinzon for their field and laboratory assistance.

Data availability

The data used in his article can be found in the CUAHSI HydroShare repository. Gonzalez-Pinzon, R. (2022). Resazurin tracer data from experiments in Colorado (2018) and Iowa (2019), HydroShare, http://www.hydroshare.org/resource/50ae3c59bebe4cb383e31408a0c10012

https://doi.org/10.5194/bg-2022-214
Preprint. Discussion started: 9 November 2022

References

Barnhart, T. B., J. Vukomanovic, P. Bourgeron, and N. P. Molotch. 2021. Future land cover and climate may drive decreases in snow wind-scour and transpiration, increasing streamflow at a Colorado, USA headwater catchment. Hydrol. Process. **35**: e14416. doi:10.1002/hyp.14416

Battin, T. J., K. Besemer, M. M. Bengtsson, A. M. Romani, and A. I. Packmann. 2016. The ecology and biogeochemistry of stream biofilms. Nat. Rev. Microbiol. **14**: 251–263. doi:10.1038/nrmicro.2016.15

Battin, T. J., L. A. Kaplan, J. D. Newbold, and C. M. E. Hansen. 2003. Contributions of microbial biofilms to ecosystem processes in stream mesocosms. Nature **426**: 439–442. doi:10.1038/nature02152

Blair, R. C., J. J. Higgins, S. Journal, and N. Winter. 1980. A Comparison of the Power of Wilcoxon ' s Rank-Sum Statistic to That of Student ' s t Statistic under Various Nonnormal Distributions Published by : American Educational Research Association and American Statistical Association Stable URL : https://www.jstor.org/stable/1164905 REFERENCES Linked references are available on JSTOR for this article : reference # references _ tab _ contents You may need to log in to JSTOR to access the linked references . **5**: 309–335.

Blume, E., M. Bischoff, J. M. Reichert, T. Moorman, A. Konopka, and R. F. Turco. 2002. Surface and subsurface microbial biomass, community structure and metabolic activity as a function of soil depth and season. Appl. Soil Ecol. **20**: 171–181. doi:10.1016/S0929-1393(02)00025-2

Bowley, A. L. 2008. The Standard Deviation of the Correlation Coefficient Author (s): A . L . Bowley Source : Journal of the American Statistical Association , Vol . 23 , No . 161 (Mar ., 1928), pp . 31- Published by : American Statistical Association Stable URL : http:/. J. Am. Stat. Assoc. **23**: 31–34.

Brooks, S. C., C. C. Brandt, and N. A. Griffiths. 2017. Estimating uncertainty in ambient and saturation nutrient uptake metrics from nutrient pulse releases in stream ecosystems. Limnol. Oceanogr. Methods **15**: 22–37. doi:10.1002/lom3.10139

Bukaveckas, P. A. 2007. Effects of Channel Restoration on Water Velocity, Transient Storage, and Nutrient Uptake in a Channelized Stream. Environ. Sci. Technol. **41**: 1570–1576. doi:10.1021/es061618x

Cardenas, M. B., J. L. Wilson, and V. A. Zlotnik. 2004. Impact of heterogeneity, bed forms, and stream curvature on subchannel hyporheic exchange. Water Resour. Res. **40**: 1–14. doi:10.1029/2004WR003008

Covino, T. P., B. McGlynn, and M. Baker. 2010a. Separating physical and biological nutrient retention and quantifying uptake kinetics from ambient to saturation in successive mountain stream reaches. J. Geophys. Res. Biogeosciences **115**: 1–17. doi:10.1029/2009JG001263

Covino, T. P., and B. L. McGlynn. 2007. Stream gains and losses across a mountain-to-valley transition: Impacts on watershed hydrology and stream water chemistry. Water Resour. Res. **43**: 1–14. doi:10.1029/2006WR005544

Covino, T. P., B. L. Mcglynn, and R. A. Mcnamara. 2010b. Tracer Additions for Spiraling Curve Characterization (TASCC): Quantifying stream nutrient uptake kinetics from ambient to saturation. Limnol. Oceanogr. Methods 484–498. doi:10.4319/lom.2010.8.484

https://doi.org/10.5194/bg-2022-214
Preprint. Discussion started: 9 November 2022

472 Covino, T. P., B. McGlynn, and J. Mallard. 2011. Stream-groundwater exchange and hydrologic
473 turnover at the network scale. Water Resour. Res. **47**: 1–11. doi:10.1029/2011WR010942
474 Dallan, E., P. Regier, A. Marion, and R. González-Pinzón. 2020. Does the Mass Balance of the
475 Reactive Tracers Resazurin and Resorufin Close at the Microbial Scale? J. Geophys. Res.
476 Biogeosciences **125**: 1–10. doi:10.1029/2019JG005435
477 Day, N. K., and R. O. Hall. 2017. Ammonium uptake kinetics and nitrification in mountain
478 streams. Freshw. Sci. **36**: 41–54. doi:10.1086/690600
479 Emanuelson, K., T. P. Covino, A. S. Ward, J. Dorley, and M. N. Gooseff. 2022. Conservative
480 solute transport processes and associated transient storage mechanisms: Comparing
481 streams with contrasting channel morphologies, land use and land cover. Hydrol. Process.
482 **36**.
483 Ensign, S. H., and M. W. Doyle. 2005. In-channel transient storage and associated nutrient
484 retention: Evidence from experimental manipulations. Limnol. Oceanogr. **50**: 1740–1751.
485 doi:10.4319/lo.2005.50.6.1740
486 Ensign, S. H., and M. W. Doyle. 2006. Nutrient spiraling in streams and river networks. J.
487 Geophys. Res. Biogeosciences **111**. doi:10.1029/2005jg000114
488 Fields, J. F., and D. P. Dethier. 2019. From on high: Geochemistry of alpine springs, Niwot
489 Ridge, Colorado Front Range, USA. Hydrol. Process. **33**: 1756–1774.
490 doi:10.1002/hyp.13436
491 Gibson, C. A., C. M. O'Reilly, A. L. Conine, and S. M. Lipshutz. 2015. Nutrient uptake
492 dynamics across a gradient of nutrient concentrations and ratios at the landscape scale. J.
493 Geophys. Res. Biogeosciences **120**: 326–340. doi:10.1002/2014JG002747
494 Gomez, J. D., J. L. Wilson, and M. B. Cardenas. 2012. Residence time distributions in sinuosity-
495 driven hyporheic zones and their biogeochemical effects. Water Resour. Res. **48**: 1–17.
496 doi:10.1029/2012WR012180
497 González-Pinzón, R., and R. Haggerty. 2013. An efficient method to estimate processing rates in
498 streams. Water Resour. Res. **49**: 6096–6099. doi:10.1002/wrcr.20446
499 González-Pinzón, R., R. Haggerty, and A. Argerich. 2014. Quantifying spatial differences in
500 metabolism in headwater streams. Freshw. Sci. **33**: 798–811. doi:10.1086/677555
501 González-Pinzón, R., R. Haggerty, and M. Dentz. 2013. Scaling and predicting solute transport
502 processes in streams. Water Resour. Res. **49**: 4071–4088. doi:10.1002/wrcr.20280
503 González-Pinzón, R., R. Haggerty, and D. D. Myrold. 2012. Measuring aerobic respiration in
504 stream ecosystems using the resazurin-resorufin system. J. Geophys. Res. Biogeosciences
505 **117**: 1–10. doi:10.1029/2012JG001965
506 González-Pinzón, R., J. Mortensen, and D. Van Horn. 2015. Comment on "Solute-specific
507 scaling of inorganic nitrogen and phosphorus uptake in streams" by Hall et al. (2013).
508 Biogeosciences **12**: 5365–5369. doi:10.5194/bg-12-5365-2015
509 González-Pinzón, R., M. Peipoch, R. Haggerty, E. Martí, and J. H. Fleckenstein. 2016.
510 Nighttime and daytime respiration in a headwater stream. Ecohydrology **9**: 93–100.
511 doi:10.1002/eco.1615
512 Gooseff, M. N., K. E. Bencala, D. T. Scott, R. L. Runkel, and D. M. McKnight. 2005. Sensitivity
513 analysis of conservative and reactive stream transient storage models applied to field data
514 from multiple-reach experiments. Adv. Water Resour. **28**: 479–492.
515 doi:10.1016/j.advwatres.2004.11.012

https://doi.org/10.5194/bg-2022-214
Preprint. Discussion started: 9 November 2022

516 Gooseff, M. N., D. M. McKnight, R. L. Runkel, and J. H. Duff. 2004. Denitrification and
517 hydrologic transient storage in a glacial meltwater stream, McMurdo Dry Valleys,
518 Antarctica. Limnol. Oceanogr. **49**: 1884–1895. doi:10.4319/lo.2004.49.5.1884
519 Gootman, K. S., R. G. Pinzón, J. L. A. Knapp, V. Garayburu-Caruso, and J. Cable. 2020.
520 Spatiotemporal Variability in Transport and Reactive Processes Across a First - to Fifth -
521 Order Fluvial Network Water Resources Research. 1–18. doi:10.1029/2019WR026303
522 Haggerty, R., M. Ribot, G. A. Singer, E. Martí, A. Argerich, G. Agell, and T. J. Battin. 2014.
523 Ecosystem respiration increases with biofilm growth and bed forms: Flume
524 measurements with resazurin. J. Geophys. Res. Biogeosciences **119**: 2220–2230.
525 doi:10.1002/2013JG002498
526 Hall, R. J. O., E. S. Bernhardt, and G. E. Likens. 2002. Relating nutrient uptake with transient
527 storage in forested mountain streams. Limnol. Oceanogr. **47**: 255–265.
528 doi:10.4319/lo.2002.47.1.0255
529 Hall, R. O., J. L. Tank, D. J. Sobota, and others. 2009. Nitrate removal in stream ecosystems
530 measured by 15N addition experiments: Total uptake. Limnol. Oceanogr. **54**: 653–665.
531 doi:10.4319/lo.2009.54.3.0653
532 Harvey, J. W., J. K. Böhlke, M. A. Voytek, D. Scott, and C. R. Tobias. 2013. Hyporheic zone
533 denitrification: Controls on effective reaction depth and contribution to whole-stream
534 mass balance. Water Resour. Res. **49**: 6298–6316. doi:10.1002/wrcr.20492
535 Harvey, J. W., J. E. Saiers, and J. T. Newlin. 2005. Solute transport and storage mechanisms in
536 wetlands of the Everglades, south Florida. Water Resour. Res. **41**.
537 doi:10.1029/2004WR003507
538 Jackson, T. R., S. V. Apte, R. Haggerty, and R. Budwig. 2015. Flow structure and mean
539 residence times of lateral cavities in open channel flows: influence of bed roughness and
540 shape. Environ. Fluid Mech. **15**: 1069–1100. doi:10.1007/s10652-015-9407-2
541 Jackson, T. R., R. Haggerty, S. V. Apte, A. Coleman, and K. J. Drost. 2012. Defining and
542 measuring the mean residence time of lateral surface transient storage zones in small
543 streams. Water Resour. Res. **48**. doi:10.1029/2012WR012096
544 Jackson, T. R., R. Haggerty, S. V. Apte, and B. L. O'Connor. 2013. A mean residence time
545 relationship for lateral cavities in gravel-bed rivers and streams: Incorporating streambed
546 roughness and cavity shape. Water Resour. Res. **49**: 3642–3650. doi:10.1002/wrcr.20272
547 Kasahara, T., and S. M. Wondzell. 2003. Geomorphic controls on hyporheic exchange flow in
548 mountain streams. Water Resour. Res. **39**: SBH 3-1-SBH 3-14.
549 doi:10.1029/2002wr001386
550 Kelleher, C., T. Wagener, B. McGlynn, A. S. Ward, M. N. Gooseff, and R. A. Payn. 2013.
551 Identifiability of transient storage model parameters along a mountain stream. Water
552 Resour. Res. **49**: 5290–5306. doi:10.1002/wrcr.20413
553 Kiel, B. A., and M. Bayani Cardenas. 2014. Lateral hyporheic exchange throughout the
554 Mississippi River network. Nat. Geosci. **7**: 413–417. doi:10.1038/ngeo2157
555 Knapp, J. L. A., R. González-Pinzón, J. D. Drummond, L. G. Larsen, O. A. Cirpka, and J. W.
556 Harvey. 2017. Tracer-based characterization of hyporheic exchange and benthic biolayers
557 in streams. Water Resour. Res. **53**: 1575–1594. doi:10.1002/2016WR019393
558 Knapp, J. L. A., R. González-Pinzón, and R. Haggerty. 2018. The Resazurin-Resorufin System:
559 Insights From a Decade of "Smart" Tracer Development for Hydrologic Applications.
560 Water Resour. Res. **54**: 6877–6889. doi:10.1029/2018WR023103

https://doi.org/10.5194/bg-2022-214
Preprint. Discussion started: 9 November 2022

561 Knapp, J. L. A., and C. Kelleher. 2020. A Perspective on the Future of Transient Storage
562 Modeling: Let's Stop Chasing Our Tails. Water Resour. Res. **56**: e2019WR026257.
563 doi:10.1029/2019WR026257
564 Krause, S., J. Lewandowski, N. B. Grimm, and others. 2017. Ecohydrological interfaces as hot
565 spots of ecosystem processes: ECOHYDROLOGICAL INTERFACES AS HOT SPOTS.
566 Water Resour. Res. **53**: 6359–6376. doi:10.1002/2016WR019516
567 Lautz, L. K., and D. I. Siegel. 2007. The effect of transient storage on nitrate uptake lengths in
568 streams: an inter-site comparison. Hydrol. Process. **21**: 3533–3548. doi:10.1002/hyp.6569
569 Li, L., P. L. Sullivan, P. Benettin, and others. 2021. Toward catchment hydro-biogeochemical
570 theories. Wiley Interdiscip. Rev. Water **8**: 1–31. doi:10.1002/wat2.1495
571 Li, Z., Z. Zeng, D. Tian, and others. 2020. The stoichiometry of soil microbial biomass
572 determines metabolic quotient of nitrogen mineralization. Environ. Res. Lett. **15**: 034005.
573 doi:10.1088/1748-9326/ab6a26
574 Liu, S., T. Maavara, C. B. Brinkerhoff, and P. A. Raymond. 2022. Global Controls on DOC
575 Reaction Versus Export in Watersheds: A Damköhler Number Analysis. Glob.
576 Biogeochem. Cycles **36**: e2021GB007278. doi:10.1029/2021GB007278
577 Martí, E., N. B. Grimm, and S. G. Fisher. 1997. Pre- and Post-Flood Retention Efficiency of
578 Nitrogen in a Sonoran Desert Stream. J. North Am. Benthol. Soc. **16**: 805–819.
579 doi:10.2307/1468173
580 Merchant, S. S., and J. D. Helmann. 2012. Elemental Economy: microbial strategies for
581 optimizing growth in the face of nutrient limitation. Adv. Microb. Physiol. **60**: 91–210.
582 doi:10.1016/B978-0-12-398264-3.00002-4
583 Mulholland, P. J., and W. R. Hill. 1997. Seasonal patterns in streamwater nutrient and dissolved
584 organic carbon concentrations: Separating catchment flow path and in-stream effects.
585 Water Resour. Res. **33**: 1297–1306. doi:10.1029/97wr00490
586 Natural Resources Conservation Service. Web Soil Survey. U. S. Dep. Agric.
587 Navel, S., F. Mermillod-Blondin, B. Montuelle, E. Chauvet, L. Simon, and P. Marmonier. 2011.
588 Water-Sediment Exchanges Control Microbial Processes Associated with Leaf Litter
589 Degradation in the Hyporheic Zone: A Microcosm Study. Microb. Ecol. **61**: 968–979.
590 doi:10.1007/s00248-010-9774-7
591 Niyogi, D. K., K. S. Simon, and C. R. Townsend. 2004. Land use and stream ecosystem
592 functioning: nutrient uptake in streams that contrast in agricultural development. Arch.
593 Für Hydrobiol. **160**: 471–486. doi:10.1127/0003-9136/2004/0160-0471
594 Ocampo, C., Oldham, C., and Sivapalan, M. 2020. Nitrate attenuation in agricultural catchments:
595 Shifting balances between transport and reaction - Ocampo - 2006 - Water Resources
596 Research - Wiley Online Library.
597 Oldham, C. E., D. E. Farrow, and S. Peiffer. 2013. A generalized Damköhler number for
598 classifying material processing in hydrological systems. Hydrol. Earth Syst. Sci. **17**:
599 1133–1148. doi:10.5194/hess-17-1133-2013
600 Peralta-Maraver, I., J. Reiss, and A. L. Robertson. 2018. Interplay of hydrology, community
601 ecology and pollutant attenuation in the hyporheic zone. Sci. Total Environ. **610–611**:
602 267–275. doi:10.1016/j.scitotenv.2017.08.036
603 Pinay, G., S. Peiffer, J.-R. De Dreuzy, and others. 2015. Upscaling Nitrogen Removal Capacity
604 from Local Hotspots to Low Stream Orders' Drainage Basins. Ecosystems **18**: 1101–
605 1120. doi:10.1007/s10021-015-9878-5
606 Ries III, K. G., J. K. Newson, M. J. Smith, and others. 2017. StreamStats, version 4.

https://doi.org/10.5194/bg-2022-214
Preprint. Discussion started: 9 November 2022

607 Rodríguez-Cardona, B., A. S. Wymore, and W. H. McDowell. 2016. DOC:NO3− ratios and
608 NO3− uptake in forested headwater streams. J. Geophys. Res. Biogeosciences **121**: 205–
609 217. doi:10.1002/2015JG003146
610 Ryan, R. J., A. I. Packman, and S. S. Kilham. 2007. Relating phosphorus uptake to changes in
611 transient storage and streambed sediment characteristics in headwater tributaries of
612 Valley Creek, an urbanizing watershed. J. Hydrol. **336**: 444–457.
613 doi:10.1016/j.jhydrol.2007.01.021
614 Schmid, B. H., I. Innocenti, and U. Sanfilippo. 2010. Characterizing solute transport with
615 transient storage across a range of flow rates: The evidence of repeated tracer
616 experiments in Austrian and Italian streams. Adv. Water Resour. **33**: 1340–1346.
617 doi:10.1016/j.advwatres.2010.06.001
618 Sheibley, R. W., J. H. Duff, and A. J. Tesoriero. 2014. Low Transient Storage and Uptake
619 Efficiencies in Seven Agricultural Streams: Implications for Nutrient Demand. J.
620 Environ. Qual. **43**: 1980–1990. doi:10.2134/jeq2014.01.0034
621 Thomas, S. A., H. Maurice Valett, J. R. Webster, and P. J. Mulholland. 2003. A regression
622 approach to estimating reactive solute uptake in advective and transient storage zones of
623 stream ecosystems. Adv. Water Resour. **26**: 965–976. doi:10.1016/S0309-
624 1708(03)00083-6
625 Trentman, M. T., W. K. Dodds, J. S. Fencl, K. Gerber, J. Guarneri, S. M. Hitchman, Z. Peterson,
626 and J. Rüegg. 2015. Quantifying ambient nitrogen uptake and functional relationships of
627 uptake versus concentration in streams: a comparison of stable isotope, pulse, and plateau
628 approaches. Biogeochemistry **125**: 65–79.
629 Valett, H. M., J. A. Morrice, C. N. Dahm, and M. E. Campana. 1996. Parent lithology, surface-
630 groundwater exchange, and nitrate retention in headwater streams. Limnol. Oceanogr. **41**:
631 333–345. doi:10.4319/lo.1996.41.2.0333
632 Ward, A. S., and A. I. Packman. 2019. Advancing our predictive understanding of river corridor
633 exchange. Wiley Interdiscip. Rev. Water **6**: e1327. doi:10.1002/wat2.1327
634 Ward, A. S., R. A. Payn, M. N. Gooseff, B. L. McGlynn, K. E. Bencala, C. A. Kelleher, S. M.
635 Wondzell, and T. Wagener. 2013. Variations in surface water-ground water interactions
636 along a headwater mountain stream: Comparisons between transient storage and water
637 balance analyses. Water Resour. Res. **49**: 3359–3374. doi:10.1002/wrcr.20148
638 Webster, J. R., P. J. Mulholland, J. L. Tank, and others. 2003. Factors affecting ammonium
639 uptake in streams - an inter-biome perspective. Freshw. Biol. **48**: 1329–1352.
640 doi:10.1046/j.1365-2427.2003.01094.x
641 Wen, H., and L. Li. 2018. An upscaled rate law for mineral dissolution in heterogeneous media:
642 The role of time and length scales. Geochim. Cosmochim. Acta **235**: 1–20.
643 doi:10.1016/j.gca.2018.04.024
644 Wondzell, S. M. 2006. Effect of morphology and discharge on hyporheic exchange flows in two
645 small streams in the Cascade Mountains of Oregon, USA. Hydrol. Process. **20**: 267–287.
646 doi:10.1002/hyp.5902
647 Zarnetske, J. P., M. N. Gooseff, T. R. Brosten, J. H. Bradford, J. P. McNamara, and W. B.
648 Bowden. 2007. Transient storage as a function of geomorphology, discharge, and
649 permafrost active layer conditions in Arctic tundra streams. Water Resour. Res. **43**: 7410.
650 doi:10.1029/2005WR004816

https://doi.org/10.5194/bg-2022-214
Preprint. Discussion started: 9 November 2022

651 Zarnetske, J. P., R. Haggerty, S. M. Wondzell, V. A. Bokil, and R. González-Pinzón. 2012.
652 Coupled transport and reaction kinetics control the nitrate source-sink function of
653 hyporheic zones. Water Resour. Res. **48**. doi:10.1029/2012wr011894
654